International Journal of Coal Science & Technology (2023) 10:16
https://doi.org/10.1007/s40789-023-00574-9

RESEARCH

# Insight into the key kinetic steps in the pyrolysis of coking and non-coking coals, characterization of the pyrolysis products

P. N. Kuznetsov[1,2] · O. Yu. Fetisova[2] · L. I. Kuznetsova[2] · B. Avid[3] · B. Purevsuren[3]

Received: 8 March 2022 / Revised: 9 June 2022 / Accepted: 10 February 2023


**Abstract**
The chemical composition, structural and plastometric properties of different-ranked coals from Mongolia deposits were studied. The non-isothermal iso-conversion Ozawa–Flynn–Wall and Friedman model-free methods were used to assess kinetic parameters and to differentiate decomposition steps. Key peculiarities of the pyrolysis kinetics of brown and bituminous coals were revealed and discussed in terms of the composition and plastometric properties. Brown coal was shown to undergo three decomposition steps with ever increasing activation energy as temperature increased because of the decomposition of thermally more and more stable molecular fragments. The pyrolysis of bituminous coals occurred in four steps, the activation energy having extreme mode of temperature dependence. An important new finding was that the temperature range of the second, major pyrolysis step well corresponded to that between the softening and re-solidification temperatures according to Gieseler plastometry. The yield and composition of the pyrolysis products obtained under isothermal conditions were also characterized depending on coal rank and temperature, and the ways for qualified utilizations were offered.

**Keywords** Coal · Pyrolysis · Thermogravimetry · Plastometry · Activation energy

## 1 Introduction

Coal continues to be one of the main sources of energy worldwide and it is indispensable in the steel-making industry. Mongolia has large reserves of coals of various grades (Erdenetsogt et al. 2009). Currently, mainly brown and subbituminous coals are utilized for heat and electricity generation. However, direct combustion results in environmental problems. Also, coking coal is currently mined at the largest Tavantolgoi deposit to export for China for the production of metallurgical coke.

Much attention is paid in Mongolia to the development of coal processing into environmentally friendly energy carriers and valuable chemical substances and carbon materials. The results of the studies of the properties of a number of low-rank coals in the processes of thermal and thermochemical conversion (Ariunaa et al. 2021; Avid et al. 2016; Purevsuren et al. 2013, 2019), gasification (Avid et al. 2016; Kuznetsov et al. 2015), and production of porous carbon materials (Gombojav et al. 2020) have been published in the literature. The coking properties of Tavantolgoi coal have been reported in Ulanovsky and Likhenko (2009), Fedorova et al. (2015). However, in general, the chemical composition and structure of Mongolian coals are still poorly investigated.

The coal pyrolysis is a fundamentally important process since it involves a set of chemical reactions, which play key roles in most coal conversion processes, such as coking, liquefaction, hydrogenation, gasification and combustion. The pyrolysis can be considered also as a test reaction for coals because of high sensitivity to coal properties. For all these reasons coal pyrolysis has been and is being studied from different perspectives (Solomon et al. 1992; Yan et al. 2020a,

✉ O. Yu. Fetisova
fou1978@mail.ru

L. I. Kuznetsova
kpn@icct.ru

B. Avid
avidmas@gmail.com

1 Institute of Petroleum and Gas, Siberian Federal University, Krasnoyarsk, Russia

2 Institute of Chemistry and Chemical Technology SB RAS, Federal Research Center "Krasnoyarsk Science Center SB RAS", Krasnoyarsk, Russia

3 Institute of Chemistry and Chemical Technology, Mongolian Academy of Sciences, Ulaanbaatar, Mongolia

Published online: 23 March 2023

b; Niksa 1991; Kandiyoti et al. 2016). Detailed information on the pyrolysis kinetics is an actual objective to better understand decomposition phenomena, to forecast chemical and physical changes and to optimize conversion into valuable products (Niksa 1991; Arenillas et al. 2001; Pretorius et al. 2017). Thermogravimetric analysis (TGA) in both isothermal and non-isothermal modes is the most common technique for studying the thermal properties and kinetics of coal pyrolysis (Arenillas et al. 2001; Fetisova et al. 2020; Kumar et al. 2021; Geng et al. 2016; Zhang et al. 2013; Xu et al. 2015). Based on the TGA measurements, a number of kinetic pyrolysis methods has been developed including model-fitting methods such as Freeman–Carroll (Liu and Fan 1999), Coats-Redfern models (Ebrahimi-Kahrizsangi and Abbasi 2008) and model-free methods such as Friedman (Friedman 1964), Kissinger–Akahira–Sunose (Mishra and Mohanty 2018), Ozawa–Flynn–Wall (Flynn and Wall 1966; Ozawa 1965; Zheng et al. 2015). Systematic trends in the kinetic parameters with coal rank and maceral composition have been found (Geng et al. 2016; Li 2007, 2013; Gao et al. 2016; Niu et al. 2016; Song et al. 2017). The pyrolysis was shown to involve the rupture of different kinds of chemical bonds, the reactions with lower bond energies occurring generally at relatively low temperatures, while those with high energies at higher temperatures.

Of the coals of different ranks, bituminous coals of medium rank have specific physical properties: at certain temperature, they can undergo a plastic state and then form strong coke at elevated temperature. Due to this valuable property, these coals are widely used in large-scale coke-making industry. However, few papers were devoted to the investigation of the pyrolysis kinetics of these coals (Du et al. 2019; Yan et al. 2020a, b). Casal et al. (2018) studied the pyrolysis kinetics of a series of bituminous coals, and also of non-bituminous coals for comparison. The pyrolysis of all the coals was reported to consist of three stages. The kinetic parameters for the main (second) decomposition stage estimated by the integral method obeyed general dependencies on the coal properties, such as rank, indexes of chemical structure. Yan et al. (2020a, b) also investigated the pyrolysis of different-ranked coals using distributed activation energy model. The activation energy values for the low-ranked coals were reported to increase gradually as coal conversion increased. However, a bituminous coal of medium rank showed an extremal varying trend of activation energy versus conversion: the initial pyrolysis stage proceeded with an ever decreasing activation energy (from 313 to 240 kJ/mol), and then, when the pyrolysis conversion has reached 40%–50%, the activation energy commenced to increase gradually as conversion further increased. Such a specific pyrolysis behavior of bituminous coal was difficult to interpret reasonably based on the presented data of chemical and molecular compositions. Perhaps, this interesting phenomenon could result from the thermoplastic properties of coal, however the relevant data were not presented.

The purpose of this paper was to study the chemical composition and structural properties of the coking and non-coking Mongolian coals, to evaluate pyrolysis kinetics and to find relations with the structural characteristics and thermoplastic properties. The kinetic parameters were estimated using the most developed and widely applied Ozawa–Flynn–Wall (OFW) and Friedman model-free methods. Also, the yield and composition of the isothermal pyrolysis products were characterized depending on the temperature and coal type.

## 2 Experimental

### 2.1 Coal samples and their chemical and structural characterization

#### 2.1.1 Sample preparation and analytical characterization

The vitrinite-type coals from the Baganuur (B), Nariinsukhait (N), and Tavantolgoi (T) deposits in Mongolia were used in this paper. The coals were ground (particle size < 0.2 mm) and dried in a vacuum oven. The contents of moisture, ash, volatile matter and vitrinite reflectance were determined using standard procedures. The fluidity characteristics (softening point and re-solidification temperature) were determined using Gieseler plastometer, and plastic layer thickness by Sapozhnikov method. Ultimate analysis was performed using a Flash EATM 1112 analyzer. The content of metals in the ash was analyzed by the X-ray fluorescence method.

#### 2.1.2 Structural characterization

The FTIR spectra were studied using KBr pellets prepared by a conventional technique (Sobkowiak and Painter 1992, 1995). The spectra were recorded on a *Nicolet 20-PC* and *Bruker Tensor-27* spectrometer within the wavenumbers of 400–4000 $cm^{-1}$. Multipoint correction of a baseline was conducted by built-in software. Based on the FTIR spectra, the semiquantitative indexes for aromaticity of hydrogen ($H_{ar}$) and carbon ($C_{ar}$) and $CH_3/CH_2$ ratio were estimated.

The X-ray diffraction patterns for the powdered coal samples packed into an aluminum holder were recorded using a PANalyticalX'Pert PRO diffractometer with Cu Kα radiation and step scanning ($2\theta = 0.2°$, 25 s/step) between $2\theta$ from 5° and 55° under strictly the same conditions. The parameters of the stacking structure of the coal matter were estimated according to recommendations (Takagi et al. 2004; Lu et al. 2001) from the (002) and (10) reflections corrected with absorption, polarization, and atomic scattering factors. The

average distance between the polyaromatic layers, $d_{002}$ was determined from the (002) peak position using Bragg's equation. The average thickness ($L_c$) of the stacks was evaluated from the width at the half-maximum of the (002) peak using Scherrer's equation, and the number of aromatic layers in the stacks by means of the equation $n=(L_c/d_{002})+1$. The average diameter of layers ($L_a$) was calculated from the width at the half-maximum of the (10).

### 2.2 Nonisothermal thermogravimetric and kinetic analysis

Thermogravimetric analysis (TGA) was carried out in a corundum crucible using a STA 449 F1 Jupiter instrument (NETZSCH) in temperature range from 30 °C to 1000 °C in an argon flow (flow rates of shielding and purge gases were 20 and 50 mL/min, respectively). The results of the measurements were processed using the NETZSCH Proteus Thermal Analysis 5.1.0 software package supplied with the instrument. The kinetic characteristics were determined based on the TGA data obtained at the heating rates of 5, 10, 15 and 20°/min. The kinetic parameters were estimated using Ozawa–Flynn–Wall (OFW) and Friedman isoconversional model-free methods which has been successfully used previously (Fetisova et al. 2020) to study the kinetics of thermal decomposition of lignin.

### 2.3 Isothermal pyrolysis of coals

The determination of the yields of pyrolysis products (char, tar, water and gases) at isothermal conditions were carried in accordance with the standard method 3168–93 (ICO 647-74) using experimental unit with a quartz retort reactor (Fig. 1). A portion of dry crushed coal (1 g, particle size less than 0.2 mm) in a pre-weighed quartz tube retort 3 was placed in an electric furnace (2). The retort was hermetically connected to another pre-weighed tube (7) (filled with glass fiber) and to flask (8). After purging with nitrogen, the retort (3) was heated to a desired temperature measured by thermocouple (1) and held for 80 min, the temperature of tube 7 being maintained at 95 °C. The tar was condensed in tube 7 on a glass fiber (coal tar), and water vapor in a cooled flask 8. he yields of solid residue (char), tar and pyrogenic water were determined from the change in the weight of tubes 3, 7 and flask 8. The yield of gases + losses was calculated from the difference.

A bench scale unit with a tubular stainless steel reactor (volume of 1.5 L) was used also to obtain larger amounts of products required for analytical measurements.

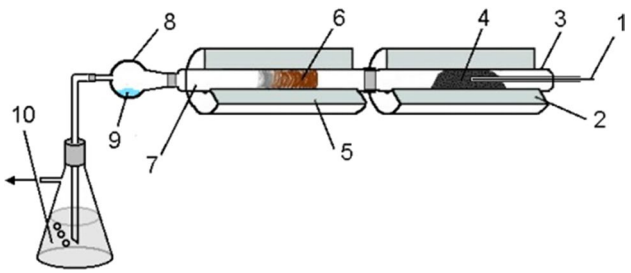


**Fig. 1** The schematic diagram of the unit for the determination of the yields of pyrolysis products under the isothermal conditions

## 3 Results and discussion

### 3.1 The composition of coals

The samples used represented vitrinite-type coals (vitrinite content of more than 75%) with a few amount of ash. Shown in Tables 1 and 2 are the data on the proximate and ultimate analysis data. N and T coals showed coking ability, their plastic layer thicknesses were 10 and 16 mm, respectively. Brown coal exhibited no coking properties. The carbon and oxygen contents ranged 70.9% to 87.8% and 22.4% to 5.4%, respectively, in accordance with $V^{daf}$ and $R_{o,r}$. All the coals showed low sulfur and nitrogen contents. These characteristics confirm the samples to correspond to brown coal (B) and two bituminous coals (N and T).

The composition of the ash from T coal was dominated by silicon (77.6%) and aluminium compounds (15.7%); from N coal – by iron (27.5%), silicon (22.8%), aluminium (17.0%) and calcium (14.8%); from B coal – by calcium (40.4%), silicon (24.2%) and iron (17.4%).

**Table 1** Proximate analysis of coal samples

| Coal | $A^d$ (wt%) | $V^{daf}$ (wt%) | $R_{o,r}$ (%) | $T_{soft}$ (°C) | $T_{res}$ (°C) | $\Delta T$ (°C) | $y$ (mm) |
|---|---|---|---|---|---|---|---|
| Baganuur (B) | 5.1 | 44.7 | 0.41 | – | – | – | – |
| Nariinsukhait (N) | 6.8 | 35.7 | 0.74 | 418 | 465 | 47 | 10 |
| Tavantolgoi (T) | 8.2 | 27.7 | 1.12 | 429 | 499 | 70 | 16 |

$R_{o,r}$ is random vitrinite reflectance; $T_{soft}$is softening temperature; $T_{res}$ is re-solidification temperature; $\Delta T$ is plasticity range; $y$ is plastic layer thickness

**Table 2** Ultimate analysis data

| Coal | wt% on daf | | | | | $H/C_{at}$ |
|---|---|---|---|---|---|---|
| | C | H | N | S | O | |
| Baganuur | 70.9 | 5.2 | 1.0 | 0.5 | 22.4 | 0.88 |
| Nariinsukhait | 84.4 | 4.8 | 1.6 | 1.0 | 8.3 | 0.68 |
| Tavantolgoi | 87.8 | 5.2 | 1.2 | 0.4 | 5.4 | 0.71 |

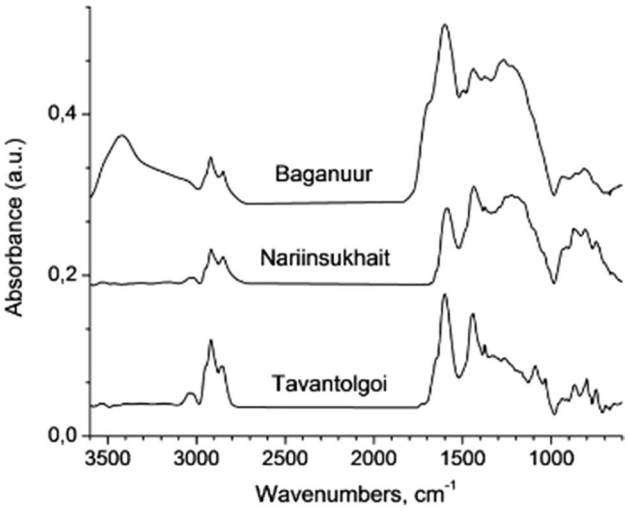


**Fig. 2** The FTIR spectra of Mongolian coals

## 3.2 Structural characterization of coals

### 3.2.1 Characterization of molecular structure by FTIR spectra

The FTIR spectra in Fig. 2 show strong absorbance at 3000–2750 $cm^{-1}$ (stretching vibration of the aliphatic C-H bonds), at 1460–1440 $cm^{-1}$ (bending vibration of $CH_2$ groups) and at 1376 $cm^{-1}$ (bending vibration of $CH_3$) indicating the presence of large amount of the aliphatic fragments. The absorbance at 1600 $cm^{-1}$ (stretching vibration of the aromatic rings), at 3050 $cm^{-1}$ (stretching vibration of the aromatic C–H bonds) and at 900–700 $cm^{-1}$ (out-of-plane bending of the aromatic C–H bonds) reflect the presence of the aromatic fragments. The absorbances centered at 3400 $cm^{-1}$, 1750–1700 $cm^{-1}$ and at 1300–1000 $cm^{-1}$ were attributed to various oxygenated fragments (phenolic hydroxyls, carbonyls, carboxyls, ester and ether groups, and alcohols). Brown coal featured with large amount of oxygen-containing groups, phenol hydroxyls, in particular (3400 $cm^{-1}$).

The characteristic absorbance at the 3100–2750 $cm^{-1}$ spectral region was deconvoluted into seven sub-bands (shown in Fig. 3). According to Sobkowiak and Painter (1992), the sub-bands at 3050 and 3020 $cm^{-1}$ were assigned to stretching vibrations of different aromatic C–H bonds, the sub-bands at 2955 and 2875 $cm^{-1}$ to asymmetric and symmetric stretching vibrations of C–H bonds in $CH_3$ methyl groups, and those at 2923 and 2848 $cm^{-1}$ to asymmetric and symmetric stretching vibrations of $CH_2$ methylene groups, respectively, and the sub-band at 2896 $cm^{-1}$ to methine groups.

Based on the deconvoluted spectra, the semi-quantitative aromaticity indexes for hydrogen ($H_{ar}$) and carbon ($C_{ar}$), and $CH_3/CH_2$ ratios were estimated. In assessing the indexes we

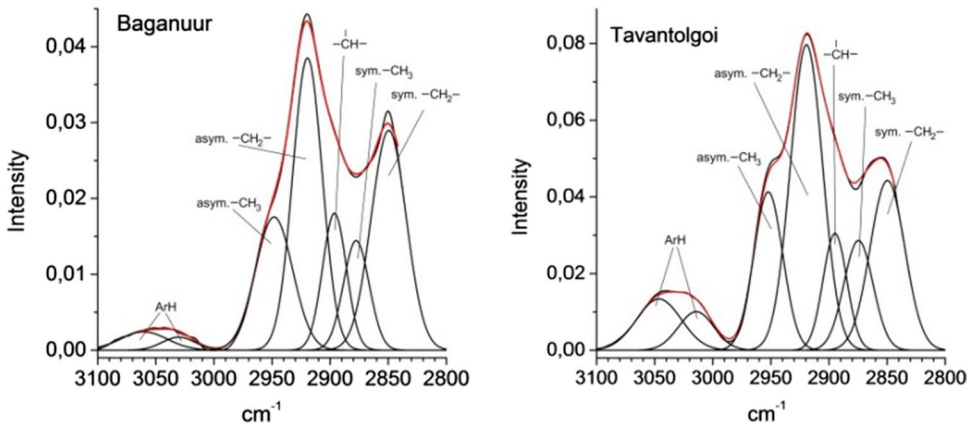


**Fig. 3** The deconvoluted FTIR spectra for Baganuur and Tavantolgoi coals as examples

**Table 3** Molecular indexes of organic matter of coals based on the FTIR spectra

| Coal | Aromaticity index | | $CH_3/CH_2$ |
|---|---|---|---|
| | $C_{ar}$ | $H_{ar}$ | |
| B | 0.66 | 0.19 | 0.29 |
| N | 0.76 | 0.36 | 0.20 |
| T | 0.76 | 0.41 | 0.23 |

took account of the statistical data for coals that the ratio of the extinction coefficient for the stretching vibrations of the aliphatic C–H bonds to the extinction coefficient for the aromatic C–H bonds is 0.20 (Sobkowiak and Painter 1992); while the ratio of the extinction coefficient for the stretching vibrations of the $CH_2$ groups and $CH_3$ groups is 0.5. The indexes were calculated using the following formulas:

$$H_{ar} = \frac{A_{ar}/0.2A_{al}}{1 + \left(A_{ar}/0.2A_{al}\right)} \quad (1)$$

$$C_{ar} = 1 - \frac{C_{al}}{C}; \frac{C_{al}}{C} = \frac{\left(\frac{H_{al}}{H} \times \frac{H}{C}\right)}{\left(\frac{H_{al}}{C_{al}}\right)} \quad (2)$$

$$CH_3/CH_2 = 0.5 \times \left(A_{2955}/A_{2923}\right) \quad (3)$$

$H_{al}/C_{al}$ in Eq. (2) is the atomic ratio of hydrogen to carbon for aliphatic groups (usually set to 2, as in methylene group) (Supaluknari et al. 1989).

Shown in Table 3 are the molecular indexes thus estimated. The values for $H_{ar}$ and $C_{ar}$ indexes decrease in the following order: Tavantolgoi–Nariinsukhait—Baganuur in accordance with $C^{daf}$, $V^{daf}$ and $R_{o,r}$. The $CH_3/CH_2$ ratios of 0.20 to 0.29 reflect different lengths of the aliphatic chains in the coals.

### 3.2.2 Characterization of the spatial coal structure

The XRD patterns for coals showed typical asymmetrical reflection in the $2\theta$ region from 8° to 34° due to intermolecular ordering of carbon matter and a weak reflection centered at $2\theta$ of about 44° due to intramolecular ordering. The curve-fitting analysis showed that the asymmetrical reflection attributed to the intermolecular ordering was best simulated by a superposition of three Gaussians which were assigned to a relatively ordered graphite-like component ($C_{graf}$) (at near $2\theta = 25°$), to less ordered $\gamma_1$-component ($2\theta$ of 19.0°–19.5°) and to least ordered $\gamma_2$-component ($2\theta$ of 10.0°–10.5°) (Fig. 4). The graphite-like component is considered usually (Speight 2015) as the stacks of the planar polycondensed aromatic clusters. Less ordered γ-components can involve mainly aliphatic fragments including naphthenes, alkanes and oxygen-containing groups spatially structured at the periphery of the graphite-like stacks.

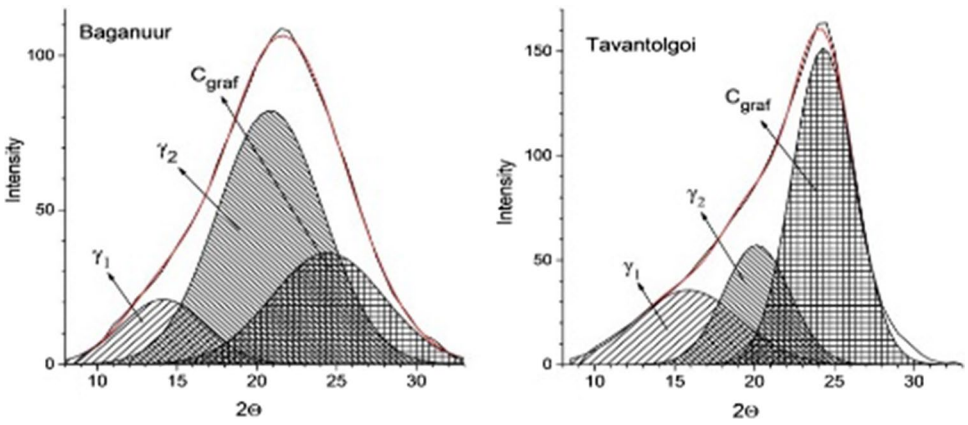


**Fig. 4** The deconvoluted fragments of the XRD patterns for Baganuur and Tavantolgoi coals

**Table 4** The characterization of the spatial structure of coals

| Coal | Proportion (%) | | Structural parameters of graphite-like component | | | | *A* (%) |
|---|---|---|---|---|---|---|---|
| | Graphite-like component | γ-component | $d_{002}$ (Å) | $L_c$ (Å) | $L_a$ (Å) | Number of layers | |
| B | 31 | 69 | 3.64 | 9.62 | 22.9 | 3.6 | 45 |
| N | 49 | 51 | 3.62 | 13.2 | 24.0 | 4.6 | 64 |
| T | 57 | 43 | 3.66 | 17.3 | 20.7 | 5.7 | 75 |

*A* refers to the proportion of the aromatic carbon atoms in the graphite-like structures

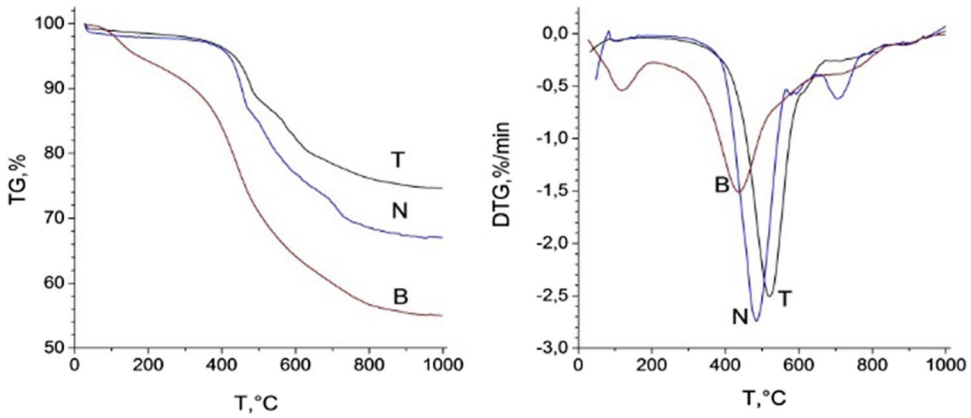


**Fig. 5** TG/DTG curves of coal pyrolysis (heating rate of 10 °C/min)

**Table 5** The thermal stability indexes of the coals derived from TG–DTG curves

| Coal | Thermal stability index (°C) | | Coke yield (wt% on daf) |
|---|---|---|---|
| | $T_{init}$ | $T_{max}$ | |
| B | 325 | 435 | 55.0 |
| N | 400 | 477 | 67.1 |
| T | 430 | 517 | 74.7 |

The parameters of the spatial structure derived from the XRD data are shown in Table 4. One can see that the spatial structure of coals contains 31% to 57% of fairly ordered graphite-like component. As the rank of coal increases, the number of layers ($n$) and the stack thickness ($L_c$) increase indicating the increase in the molecular ordering of the structure, the interlayer spacing ($d_{002}$) and layer diameter ($L_a$) remaining practically unchanged.

The proportion of the graphite-like component in the coal matter is generally considered to reflect coal aromaticity (Speight 2015). It can be drawn from comparison of $C_{ar}$ values (in Table 3) and the proportion of the graphite-like component (in Table 4) that the latter in the brown coal contained only 45% of all the aromatic carbon atoms, and the remaining aromatic carbons occur in the amorphous γ-components (possibly, in small and/or in highly substituted aromatic cycles). The polycondensed clusters in the bituminous N and T coals contain 64% and 75% of all the aromatic carbon atoms, respectively.

### 3.3 Non-isothermal pyrolysis of coals, TG/DTG results

Figure 5 shows the thermogravimetric (TG) and differential thermogravimetric (DTG) curves which reflect the temperature dependence of weight loss and the rate of weight loss, respectively.

The thermal stability indexes $T_{init}$ (temperature at the initial evolution of the volatile substances) and $T_{max}$ (temperature at maximum rate of weight loss) were estimated based on the curve analyses. It can be seen from Table 5 that both $T_{init}$ and $T_{max}$ increase in order from B to N and to T coals, indicating that coals with more aromatic and more ordered structures are more stable, hence, higher temperature is required for decomposition. These results are

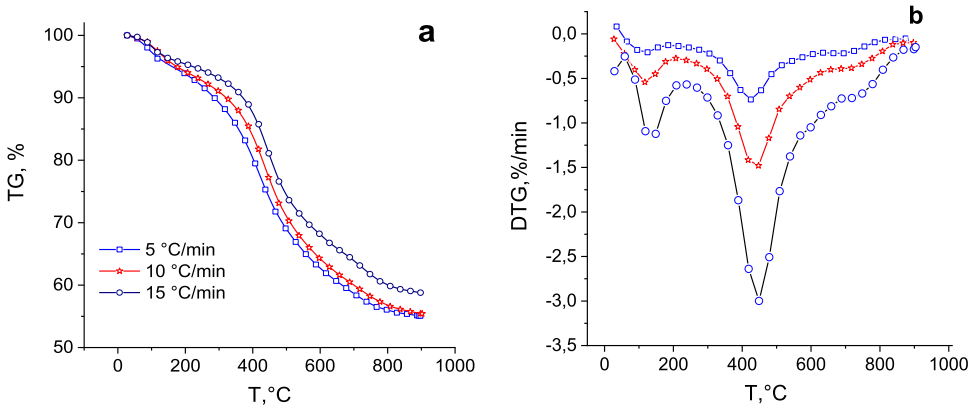


**Fig. 6** **a** TG and **b** DTG pyrolysis curves of Baganuur coal at different heating rates

consistent with the data reported in Geng et al. (2016) and Casal et al. (2018).

Figure 6 shows the TG and DTG curves obtained with different heating rate for brown coal. One can see that the increase in heating rate results in increase in the yield of coke residue and also in displacement of maximum weight loss to higher temperatures. These effects are consistent with the results reported by several authors (Ashraf et al. 2019; Konwar and Nath 2019; Du et al. 2016; Guo et al. 2018 and Zhang et al. 2013). However, generally, its nature was not discussed. Some authors consider this effect in term of a thermal hysteresis phenomenon (Du et al. 2016) or due to thermal lag (Guo et al. 2018; Zhang et al. 2013) as heating rate increases. We tend to consider that a shift of the maximum pyrolysis temperature in Fig. 6 towards higher temperatures as the heating rate increases was due to the kinetic peculiarities of some pyrolysis reactions. This phenomenon can result from different residence time of the reactants at a certain temperature. At a low heating rate, some reactions have sufficient time to be completed at certain temperature. However, at a high heating rate, the residence time is smaller, can be not sufficient for reactions to be completed, and they are rapidly completed further at a higher temperature.

The dynamics of the pyrolytic decomposition of coals is considered generally (Solomon et al. 1992) in terms of a stepwise process which involves a gradual cleavage of different chemical bonds which need corresponding activation energies for breaking. The kinetic parameters were estimated using the most developed and widely applied the isoconversional Ozawa–Flynn–Wall (OFW) model-free method as well Friedman method.

In the OFW method, the activation energy is estimated from the following generalized expression for the rate of solid-phase reaction under non-isothermal conditions:

$$\frac{\mathrm{d}\alpha}{\mathrm{d}t} = k\mathrm{f}(\alpha) = \frac{\mathrm{A}}{\beta} e^{\frac{-E_a}{RT}} f(\alpha), \tag{4}$$

where $\mathrm{d}\alpha/\mathrm{d}t$ is the rate of change of conversion ($\alpha$) with time ($t$), $A$ is the pre-exponential factor ($\mathrm{min}^{-1}$), $\beta$ is the heating rate (°C/min), $E_a$ is the apparent activation energy (J/mol), $R$ is the universal gas constant (8.314 J/mol K), $T$ is temperature (K), $f(\alpha)$ is the reaction model which is a function of conversion. Relative degree of coal conversion α can be defined as $\alpha = \frac{m_s - m}{m_s - m_f}$, where $m_s$ and $m_f$ are the initial and final weights of a sample, and $m$ is its weight at a point of measurement. The integration of Eq. (3) after rearrangement yields the integral form of non-isothermal rate law given as follows:

$$\mathrm{g}(\alpha) = \int_0^{\alpha} \frac{d\alpha}{f(\alpha)} = \int_0^{T} \frac{\mathrm{A}}{\beta} exp\left(\frac{-E}{RT}\right) \mathrm{d}T \tag{5}$$

The fundamental expressions of kinetic methods to evaluate kinetic parameters from TGA data are based on the eqs. 4 and 5.

Isoconversional methods are based on the principle that at a constant extent of conversion, the reaction rate is a function only of the temperature. Thus

$$\left[\frac{\mathrm{d}\ln\left(\frac{\mathrm{d}\alpha}{\mathrm{d}t}\right)}{\mathrm{d}T^{-1}}\right]_{\alpha} = -\frac{E_{\alpha}}{R} \tag{6}$$

Ozawa–Flynn–Wall method (Flynn and Wall 1966; Ozawa 1965) can be defined by the following equation:

$$\ln\beta = \ln\left[\frac{\mathrm{A}E_{\alpha}}{Rg(\alpha)}\right] - 5.331 - 1.052\frac{E_{\alpha}}{RT} \tag{7}$$

where $\mathrm{g}(\alpha)$ is a constant at a given $\alpha$ conversion degree. By plotting ln $\beta$ versus $1/T$, the apparent activation energy $E_a$ can be calculated based on slope.

It can be seen from Fig. 7 that isoconversion lines have various slopes which indicate different activation energies. The Arrhenius approximation have high correlation coefficients ($R^2 > 0.98$). Less approximation ($R^2 = 0.83$) is observed for the initial low temperature conversion ($\alpha$ conversion of 0.1) of brown coal only. This can result from the high content of the reactive oxygen-containing groups

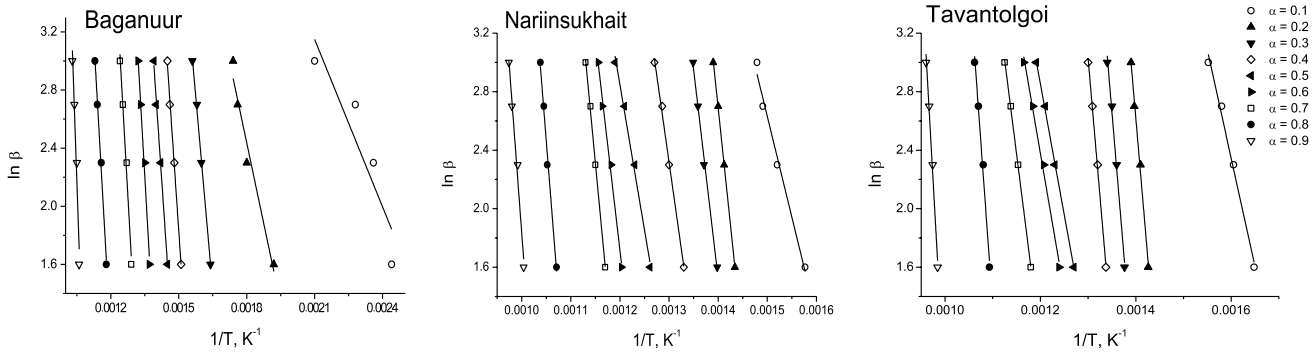


**Fig. 7** Arrhenius plots of coals with OFW method

(phenolic, acid, ether and esters groups) in brown coal compared to bituminous coals. Already at the initial stage, these groups easily enter into both endothermic destructive reactions with the release of volatiles and also exothermic polycondensation reactions with the formation of non-volatile products. These reactions can differ in activation energies, that could lead to some scatter in the values of apparent activation energies on the Arrhenius plot. However, this effect was not observed at the next steps, since these reactive functional groups have been consumed.

The similar results were obtained also by using the Friedman method. Its description and kinetic data obtained are in the Supplementary Materials (Fig. S1 and Table S1).

Plotted in Fig. 8 are the $E_a$ values calculated by OFW and Friedman methods as a function of $\alpha$, a degree of thermal decomposition of coal matter. One can see that coals show different kinetic behavior. However, a general trend is that the initial pyrolysis stages at low temperature proceeded with low apparent activation energies, and the last stages at higher temperature did with high activation energy. This phenomenon has a chemical background since the apparent activation energy is a fundamental kinetic parameter which reflects the mechanism of reaction, the nature of the rate limiting step and the consequence between the values of the activation energy and dissociation energy for separate bond is generally observed (Wanzl 1988).

Based on the profiles of the curves for activation energies, the pyrolysis process can be represented as consisting of several temperature stages (Table 6). The pyrolysis of B coal occurred via three main steps. The initial decomposition reactions at the first step started with low activation energies (33–60 kJ/mol), close to that of 35 kJ/mol reported by Casal et al. (2018) for the lignite pyrolysis at the first step. This may include primarily dissociation of hydrogen bonding and cleavage of the weakest oxygen-containing bonds. As temperature further increased, the pyrolysis proceeded with ever higher activation energy; that is, the thermally more and more stable molecular fragments were involved in the decomposition reactions. However, at temperature of 413 °C, the activation energy attained about 200 kJ/mol and then changed little up to 532 °C, that is in agreement with recently reported data by Zhang et al. (2013). The close values of the activation energies at this temperature range appears to indicate radical decomposition reactions involving some chemical bonds with a close bonding energy (Shi et al. 2013; Wanzl 1988). The last pyrolysis step occurred with ever higher and higher activation energy, it can involve predominantly endothermic dehydrogenation, deoxygenation, dealkylation and also exothermic polycondensation and restructuring of solid char to some extent.

**Table 6** The temperature ranges for the coal pyrolysis steps

| Coal | Temperature steps (°C) | | | |
|---|---|---|---|---|
| | I | II | III | 1 V |
| B | 208–413 | 413–532 | 532–707 | – |
| N | 387–428 | 428–445 | 445–496 | 496–745 |
| T | 342–427 | 427–472 | 472–514 | 514–745 |

The pyrolysis of the bituminous coals consisted of four steps. The first step proceeded with higher activation energies compared to those for B coal. This could reflect the fact that they contain progressively lower quantities of oxygen functional groups with weakest C–O bonds. As temperature increased, increasingly ever more stronger bonds were involved into destruction. However, when decomposition degree for the T coal has attained 0.2 the next pyrolysis step at temperature range of 427–472 °C occurred with a fairly constant activation energy (about 330 kJ/mol). We attribute this primarily to rupture at the rate limiting steps of some chemical bonds of approximately same strength.

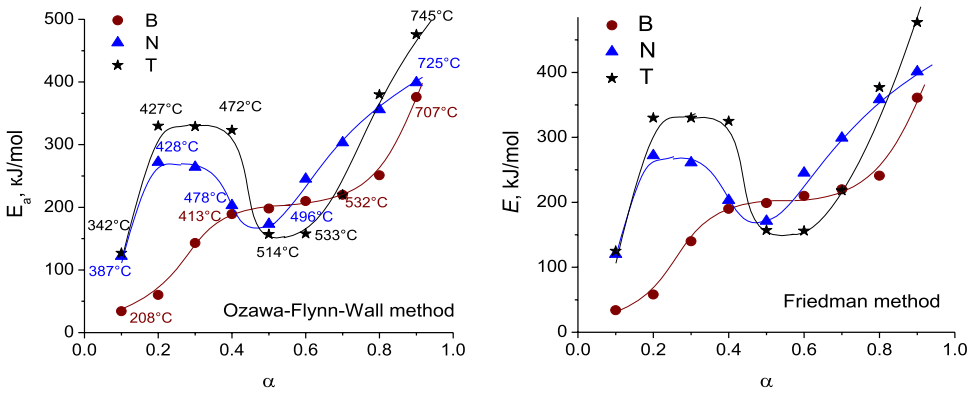


**Fig. 8** The plot of activation energies calculated by Ozawa–Flynn–Wall and Friedman methods for pyrolysis of different coals vs coal conversion

According to Gieseler plastometry, T and N bituminous coals passed at this temperature range into a fluid-like metaplastic state due to low-volatile substances resulted from the decomposition reactions, as well as due to initially present bitumen. The comparison of the temperature indicators in Tables 1 and 6 (Fig. 8) shows that for both bituminous coals there is an accordance between the temperature range of the second kinetic pyrolysis step and the softening and re-solidification temperature range. The high activation energy (330 kJ/mol and 270 kJ/mol for T and N coals, respectively) at this step reflects the endothermic nature of the reactions which may involve coal softening and extensive destructive disintegration of the organic coal matter into a molecular non-volatile metaplast and volatile substances (aromatic and aliphatic liquids. and gases). Coal softening is a consequence of both physical melting process and pyrolysis breakdown of the coal matrix, the activation energy can vary from 42 kJ/mol (Fong et al. 1985, 1986) to 210–420 kJ/mol (Waters 1962; Habermehl et al. 1981; Fitzgerald 1956). In general, this second step may include the cleavage of the chemical bonds with a similar bonding energy, which may be represented by some C–C bonds, involving aliphatic linkages between the aromatic units (Shi et al. 2013; Wanzl 1988). The softening point and the temperature range of plasticity are to be important indicators of the coking capacity of coals. Thus, it can be concluded that the pyrolysis kinetics confirmed the higher coking ability of T coal compared to N coal.

However, once decomposition degree for bituminous coals has neared to 0.4, the activation energy dropped greatly (from 330 to 150 kJ/mol, and from 230 to 170 kJ/mol, for T and N coals, respectively). This third decomposition step with a reduced activation energy could involve primarily polycondensation reactions in the metaplast matter, initiation of the nucleation reactions followed by re-solidification and generation of solid char. The polycondensation and re-solidification reactions are usually highly exothermic in nature (Solomon et al. 1992) and, hence, could proceed with a reduced activation energy. The last pyrolysis step occurred with ever higher activation energy. Primarily highly endothermic dehydrogenation, deoxygenation, dealkylation, and also polycondensation and restructuring of solid char to some extents could proceed at this high temperature step (Zhang et al. 2013).

Plotted in Fig. 9 are the $T_{max}$ and $T_{init}$ thermal stability indexes for different coals and the activation energies for the second major pyrolysis step as functions of $V^{daf}$. It can be seen that the kinetic pyrolysis indexes for both brown and bituminous coals proved to be in common, close to linear, dependences on the $V^{daf}$ yield, the lower is the rank of coal, the lower is the activation energy of pyrolysis and temperatures of the initial pyrolysis and of the maximum pyrolysis rate. This result is consistent with the data reported by Casal et al. (2018).

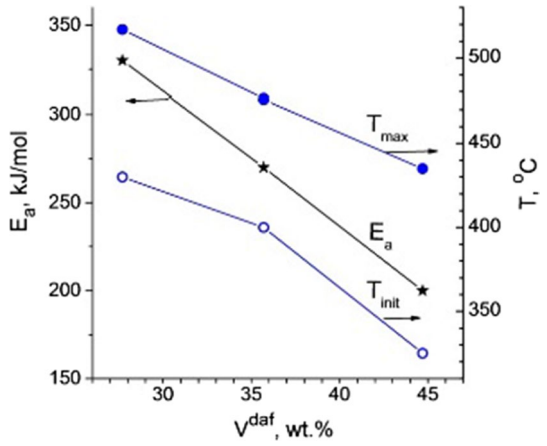


**Fig. 9** The relations between the $V_{daf}$ for coals and pyrolysis indexes $T_{max}$, $T_{init}$ and $E_a$ for the second pyrolysis stage

## 3.4 Isothermal coal pyrolysis tests

Shown in Fig. 10 are the yields of the coke residue, liquid tar and gases obtained from the isothermal pyrolysis of different coals at the temperatures of 500, 600 and 700 °C.

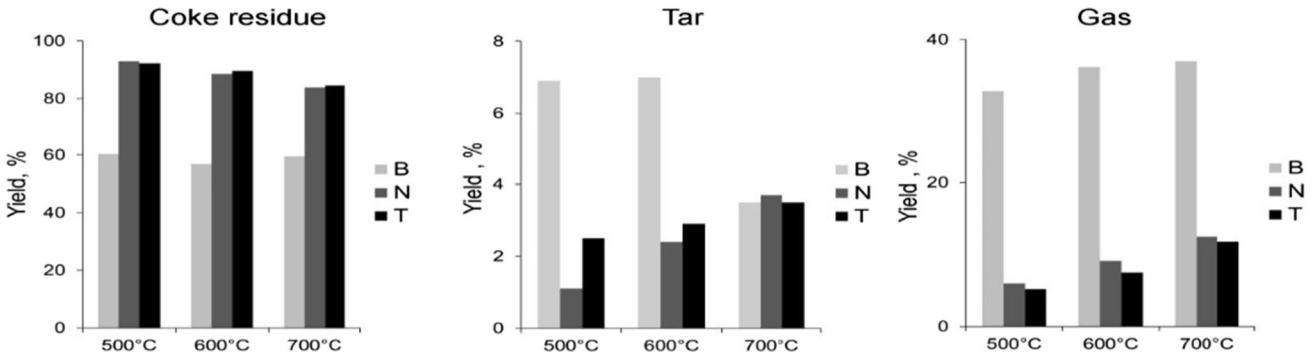


**Fig.10** The yields of products from the pyrolysis of coals at different temperatures

**Table 7** The molecular FTIR spectral indexes for pyrolysis tars

| Coal | $H_{ar}$ index | $CH_3/CH_2$ |
|---|---|---|
| B | 0.13 | 0.28 |
| N | 0.25 | 0.31 |
| T | 0.28 | 0.33 |

**Table 8** Group composition of pyrolysis tars

| Coal | Group composition (wt%) | | | | |
|---|---|---|---|---|---|
| | Bases | Acids | Phenols | Asphaltenes | Neutral oils |
| B | 3.0 | 2.0 | 14.2 | 19.2 | 61.6 |
| N | 1.1 | 2.7 | 3.2 | 12.5 | 80.5 |
| T | 1.2 | 1.2 | 3.3 | 18.8 | 75.5 |

Brown coal, compared to bituminous coals with more aromatic and ordered structure, yielded less coke residue (58%–60% *vs.* 83%–93%) and much more gases (32%–37% *vs.* 5.0%–12.5%) at whole temperature range of 500–700 °C and more tar (6.8%–7.0%) at lowered temperature range of 500–600 °C.

The liquid tars were characterized by the FTIR spectra, group analyses and by fractionation distillation. The FTIR spectra showed strong absorbances at 3000–2750 $cm^{-1}$, 1460–1440 $cm^{-1}$ and 1378 $cm^{-1}$ characteristic of the aliphatic structures. The absorbances centered at 3025 $cm^{-1}$, 1600 $cm^{-1}$ and 900–700 $cm^{-1}$ indicated aromatic structures. The oxygen-containing compounds were indicated by the absorbances centered at 3400 $cm^{-1}$, 1620–1750 $cm^{-1}$ and 1000–1200 $cm^{-1}$, the brown coal tar featured with more content of oxygen-containing substances compared to other once. The semi-quantitative FTIR molecular indexes in Table 7 show the tars from the bituminous coals to be of higher aromaticity compared to brown coal tar, and the absorption profiles in the 900–700 $cm^{-1}$ region indicated polycondensed nature.

Shown in Table 8 are the data on the group composition of coal tars. The predominant part was represented by the neutral oils, the largest part of 80.5% being characteristic of the tar from the N coal. Asphaltenes and phenols were present with less amounts, and the organic acids and bases accounted for no more than 2.5%–5.0%.

According to distillation, the brown coal oil consisted of 82.6% of gasoline and kerosene fractions and 17.4% of the non-volatile residue. The oil from the bituminous N coal contained much less distillate fraction (26.5%), the main part (73.5%) accounted for non-volatile residue. The oil from the T coal was distinguished by high viscosity, only little gasoline was distilled off, and non-volatile residue represented a pitch-like solid matter at ambient temperature. Thus, one can suggest based on the data obtained that the development of the polycondensation reactions between the non-volatile polycondensed aromatic components of the metaplast matter during the third step of pyrolysis of bituminous coals (at 470–520 °C) were the reason why these coals yielded more char and less tar compared to brown coal.

The data on the product yields, group and fractional composition of the tars obtained from the pyrolysis of different coals make it possible to optimize the pyrolysis process to obtain the targeted products. The chars produced differed from the original coals with much less volatiles (6% to 16%) and with higher calorific values (6800 to 8200 kcal/kg). Therefore, they can be used as a smoke-less and high-calorific solid fuel with a lower emission of greenhouse and harmful gases (especially important for Mongolia), as a metal reducing agent in pyrometallurgy, in iron- and steel-making, in ferroalloy production, and as a feedstock for the manufacturing of carbon materials for various needs. The distillate fractions of brown coal oil can serve as a feedstock for valuable chemicals. Also, they can be catalytically hydrotreated to produce motor fuels. The pitch-like residue from the distillation of the neutral oils can be used as a binding agent.

## 4 Conclusions

(1) The chemical composition, structural and plastometric properties of typical brown and bituminous coals from Mongolia deposits were characterized by different techniques. Their pyrolysis behaviors were studied using the non-isothermal and isothermal methods and the results were discussed in terms of the chemical, physical and plastometric properties.

(2) Key stages of the pyrolysis of brown and bituminous coals were revealed based on the kinetic parameters determined using the iso-conversion Ozawa–Flynn–Wall and Friedmen methods. The brown coal was shown to undergo three solid-phase decomposition steps, the first and third ones proceeding with an ever higher activation energy as temperature increased because of the decomposition of thermally more and more stable molecular fragments.

(3) The pyrolysis of the bituminous coals differed with a more complicated kinetics, it occurred in four steps, the activation energy having extreme mode of temperature dependence. An important new finding was that the temperature range of the second, major pyrolysis step well corresponded to that between the softening and resolidification temperatures according to Gieseler plastometry.

(4) The yield and composition of the pyrolysis products obtained under isothermal conditions were character-

ized depending on coal rank and temperature. Compared to brown coal, bituminous coals yielded significantly more char and less gases and liquid tars. The latter consisted of polycondensed aromatic substances. The ways for qualified utilizations of pyrolysis products were offered.

**Supplementary Information** The online version contains supplementary material available at https://doi.org/10.1007/s40789-023-00574-9.

**Acknowledgements** This work was funded by the framework of the State Assignment (FWES-2021-0014) for the Institute of Chemistry and Chemical Technology SB RAS using the instruments of the Krasnoyarsk Regional Research Equipment Centre of SB RAS. We declare that we have no financial and personal relationships with other people or organizations that can inappropriately influence our work. There is no professional or other personal interest of any nature or kind in any product, service and/or company that could be construed as influencing the position presented in the manuscript entitled "Insight into the key kinetic steps in the pyrolysis of coking and non-coking coals, characterization of the pyrolysis products".

**Author contributions** PNK: Investigation, Supervision Writing-Reviewing and Editing; OYF: Investigation, Data curation, Writing-Original draft preparation; LIK: Writing-Reviewing and Editing; BA: Data curation, Investigation; BP: Investigation, Supervision. All authors read and approved the final manuscript.

## Declarations

**Competing interests** The authors declare no competing financial interests or personal relationships that could influence the work reported in this paper.



## References

Arenillas A, Rubiera F, Pevida C, Pis J (2001) A comparison of different methods for predicting coal devolatilisation kinetics. J Anal Appl Pyrol 58–59:685–701. https://doi.org/10.1016/S0165-2370(00)00183-2

Ariunaa A, Zongqing B, Jin B, Narangerel J, Purevsuren B, Zhihao F, Ranran H, Chong H (2021) Thermal behavior of Mongolian low-rank coals during pyrolysis. Carbon Resour Convers 4:19–27. https://doi.org/10.1016/j.crcon.2021.01.005

Ashraf A, Sattar H, Munir S (2019) Thermal decomposition study and pyrolysis kinetics of coal and agricultural residues under non-isothermal conditions. Fuel 235:504–514

Avid B, Purevsuren B, Temuujin J (2016) Bituminous coals of Mongolia: occurrence and characteristics. Advances in Energy Research 22:159–178

Casal MD, Vega MF, Diaz-Faes E, Barriocanal C (2018) The influence of chemical structure on the kinetics of coal pyrolysis. Int J Coal Geol 195:415–422. https://doi.org/10.1016/j.coal.2018.06.014

Du R-L, Wu K, Xu D-A, Chao C-Y, Zhang L, Du X-D (2016) A modified Arrenius equation to predict the reaction rate constant of Anyuan pulverized-coal pyrolysis at different heating rates. Fuel Proc Technol 148:295–301. https://doi.org/10.1016/j.fuproc.2016.03.011

Du W, Wang G, Wang Y, Liu X (2019) Thermal degradation of bituminous coal with both model-free and model-fitting methods. Appl Therm Eng 152:169–174. https://doi.org/10.1016/j.applthermaleng.2019.02.092

Ebrahimi-Kahrizsangi R, Abbasi MH (2008) Evaluation of reliability of Coats-Redfern method for kinetic analysis of non-isothermal TGA. T Nonferr Metal Soc 18:217–221. https://doi.org/10.1016/S1003-6326(08)60039-4

Erdenetsogt B-O, Lee I, Bat-Erdene D, Jargal L (2009) Mongolian coal-bearing basins: geological settings, coal characteristics, distribution, and resources. Int J Coal Geol 80:87–104. https://doi.org/10.1016/j.coal.2009.08.002

Fedorova NI, Manina TS, Ismagilov ZR, Avid B (2015) Composition and technological properties of coal from the Tavantolgoi deposit in Mongolia. Solid Fuel Chem 49:129–134. https://doi.org/10.3103/S0361521915030064

Fetisova OY, Mikova NM, Taran OP (2020) Evaluation of the validity of model-fitting and model-free methods for kinetic analysis of nonisothermal pyrolysis of Siberian Fir Bark. Kinet Catal 61:846–853. https://doi.org/10.1134/S0023158420050043

Fitzgerald D (1956) The Kinetics of Coal Carbonization in the Plastic State. Fuel 35:178

Flynn JH, Wall LA (1966) A quick, direct method for the determination of activation energy from thermogravimetric data. J Polym Sci Part B Polym Lett 4:323–328. https://doi.org/10.1002/POL.1966.110040504

Fong WS, Peters WA, Howard JB (1985) Apparatus for determination high-temperature, high-pressure coal plastic behavior under rapid heating conditions. Rev Sci Inst 56:586. https://doi.org/10.1063/1.1138293

Fong WS, Khalil YF, Peters WA, Howard JB (1986) Plastic behavior of coal under rapid-heating high-temperature conditions. Fuel 65(2):195–201. https://doi.org/10.1016/0016-2361(86)90006-2

Friedman HL (1964) Kinetics of thermal degradation of char-forming plastic from thermogravimetry: application to a phenolic plastic. J Polym Sci Part C Polym Symp 6:183–195. https://doi.org/10.1002/polc.5070060121

Gao Z, Zheng M, Zhang D, Zhang W (2016) Low temperature pyrolysis properties and kinetics of non-coking coal in Chinese western coals. J Energy Inst 89:544–559. https://doi.org/10.1016/j.joei.2015.07.002

Geng C, Li S, Yue C, Ma Y (2016) Pyrolysis characteristics of bituminous coal. J Energy Inst 89:725–730. https://doi.org/10.1016/j.joei.2015.04.004

Gombojav U, Jambal I, Byambajav E (2020) Preparation of activated carbons from Mongolian lignite and sub-bituminous coal by a physical method. J Miner Mater Character Eng 8:97–106. https://doi.org/10.4236/jmmce.2020.83007

Guo L, Zuo H, Wang Y, Zhao J (2018) Thermal behavior and kinetics study on the pyrolysis of lean coal blend with thermally dissolved coal. J Therm Anal Calorim 136:903–912. https://doi.org/10.1007/s10973-018-7719-4

Habermehl D, Orywal F, Beyer HD (1981) "Plastic properties of Coal" in Chemistry of Coal utilization, vol 2. Wiley, New York

Kandiyoti R, Herod A, Bartle K (2016) Solid fuels and heavy hydrocarbon liquids. Thermal characterization and analysis, 2nd edn. Elsevier, Amsterdam

Konwar K, Nath HP (2019) Effect of biomass addition on the devolatilization kinetics, mechanisms and thermodynamics of a northeast Indian low rank sub-bituminous coal. Fuel 256:115926

Kumar M, Akhtar AM, Kumar V, Liu S, Li C-Z, Vuthaluru H (2021) Studies into the kinetic compensation effects of loy yang brown coal during gasification in a steam environment—a mechanistic view. Chem Eng J Adv 8:100159. https://doi.org/10.1016/j.ceja.2021.100159

Kuznetsov PN, Kolesnikova SM, Kuznetsova LI, Tarasova LS, Ismagilov ZR (2015) Steam gasification of Mongolian coals. Solid Fuel Chem 49:80–86. https://doi.org/10.3103/S0361521915020068

Li C-Z (2007) Some recent advances in the understanding of the pyrolysis and gasification behaviour of Victorian brown coal. Fuel 86:1664–1683. https://doi.org/10.1016/j.fuel.2007.01.008

Li C-Z (2013) Importance of volatile—char interactions during the pyrolysis and gasification of low-rank fuels—a review. Fuel 112:609–623. https://doi.org/10.1016/j.fuel.2013.01.031

Liu NA, Fan WC (1999) Critical consideration on the Freeman and Carroll method for evaluating global mass loss kinetics of polymer thermal degradation. Thermochim Acta 338:85–94. https://doi.org/10.1016/S0040-6031(99)00197-5

Lu L, Sahajwalla V, Kong C, Harris D (2001) Quantitative X-ray diffraction analysis and its application to various coals. Carbon 39:1821–1833. https://doi.org/10.1016/S0008-6223(00)00318-3

Mishra RK, Mohanty K (2018) Pyrolysis kinetics and thermal behavior of waste sawdust biomass using thermogravimetric analysis. Bioresour Technol 251:63–74. https://doi.org/10.1016/j.biortech.2017.12.029

Niksa S (1991) FLASHCHAIN theory for rapid coal devolatilziation kinetics: 3. Modeling the behavior of various coals. Energy Fuels 5:673–683. https://doi.org/10.1021/ef00029a008

Niu Z, Liu G, Yin H, Zhou C, Wu D, Yousaf B, Wang C (2016) In-situ FTIR study of reaction mechanism and chemical kinetics of a Xundian lignite during non-isothermal low temperature pyrolysis. Energy Convers Manage 124:180–188. https://doi.org/10.1016/j.enconman.2016.07.019

Ozawa T (1965) A new method of analyzing thermogravimetric data. Bull Chem Soc Jpn 38:1881–1886. https://doi.org/10.1246/BCSJ.38.1881

Pretorius GN, Bunt JR, Gräbner M, Neomagus H, Waanders FB, Everson RC, Strydom CA (2017) Evaluation and prediction of slow pyrolysis products derived from coals of different rank. J Anal Appl Pyrol 128:156–167. https://doi.org/10.1016/j.jaap.2017.10.014

Purevsuren B, Davaajav Y, Batbilig S, Namkhainorov J, Karaca F, Morgan TJ, Rodriguez PA, Tay FH, Kazarian S, Herod AA, Kandiyoti R (2013) Characterization of tars from the thermal processing of Baganuur and Tavan Tolgoi coals from Mongolia, using SEC, UV-F, IR and mass spectrometry. Adv Chem Eng Sci 3:130–144. https://doi.org/10.4236/aces.2013.32016

Purevsuren B, Batbileg S, Kuznetsova LI, Batkhishig D, Namkhainorov G, Kuznetsov PN (2019) Properties of coal from the bayantig deposit in Mongolia and semicoking products. Solid Fuel Chem 53:65–70. https://doi.org/10.3103/S0361521919020101

Shi L, Liu Q, Guo X, Wu W, Liu Z (2013) Pyrolysis behavior and bonding information of coal—a TGA study. Fuel Process Technol 108:125–132. https://doi.org/10.1016/j.fuproc.2012.06.023

Sobkowiak M, Painter PC (1992) Determination of the aliphatic and aromatic CH contents of coals by FT-IR: studies of coal extracts. Fuel 71:1105–1125. https://doi.org/10.1016/0016-2361(92)90092-3

Sobkowiak M, Painter PC (1995) A comparison of DRIFT and KBr pellet methodologies for the quantitative analysis of functional groups in coal by infrared spectroscopy. Energy Fuels 9:359–363. https://doi.org/10.1021/EF00050A022

Solomon PR, Serio MA, Suuberg EM (1992) Coal pyrolysis: experiments, kinetic rates and mechanisms. Prog Energy Combust 18:133–220. https://doi.org/10.1016/0360-1285(92)90021-R

Song H, Liu G, Zhang J, Wu J (2017) Pyrolysis characteristics and kinetics of low rank coals by TG-FTIR method. Fuel Process Technol 156:454–460. https://doi.org/10.1016/j.fuproc.2016.10.008

Speight JG (2015) Handbook of coal analysis, 2nd edn. Wiley, New Jersey

Supaluknari S, Larkins FP, Redlich P, Jackson WR (1989) Determination of aromaticities and other structural features of Australian coals using solid state $^{13}C$ NMR and FTIR spectroscopies. Fuel Process Technol 23:47–61. https://doi.org/10.1016/0378-3820(89)90043-X

Takagi H, Maruyama K, Yoshizawa N, Yamada Y, Sato Y (2004) XRD analysis of carbon stacking structure in coal during heat treatment. Fuel 83(17–18):2427–2433. https://doi.org/10.1016/j.fuel.2004.06.019

Ulanovsky ML, Likhenko AN (2009) The change of mineral composition coals at enrichment and coking. Coke and Chemistry 6:13–20. https://doi.org/10.3103/S1068364X09060040

Wanzl W (1988) Chemical reactions in thermal decomposition of coal. Fuel Process Technol 20(317–336):317

Waters PL (1962) Rheological properties of coal during the early stage of thermal softening. Fuel 41:3

Xu Y, Zhang Y, Zhang G, Guo Y, Zhang J, Li G (2015) Pyrolysis characteristics and kinetics of two Chinese low-rank coals. J Therm Anal Calorim 122:975–984. https://doi.org/10.1007/s10973-015-4801-z

Yan J, Liu M, Feng Z, Bai Z, Shui H, Li Z, Lei Z, Wang Z, Ren S, Kang S, Yan H (2020a) Study on the pyrolysis kinetics of low-medium rank coals with distributed activation energy model. Fuel 261:116359. https://doi.org/10.1016/j.fuel.2019.116359

Yan J, Yang Q, Zhang L, Lei Z, Li Z, Wang Z, Ren S, Kang S, Shui H (2020b) Investigation of kinetic and thermodynamic parameters of coal pyrolysis with model-free fitting methods. Carbon Resour Convers 3:173–181. https://doi.org/10.1016/j.crcon.2020.11.002

Zhang S, Zhu F, Bai C, Wen L, Zou C (2013) Thermal behavior and kinetics of the pyrolysis of the coal used in the COREX process. J Anal Appl Pyrolysis 104:660–666. https://doi.org/10.1016/j.jaap.2013.04.014

Zheng W, Liu L, Zhao XY, He JW, Wang A, Chan TW, Wu S (2015) Effects of lanthanum complex on the thermo-oxidative aging of natural rubber. Polym Degrad Stab 120:377–383. https://doi.org/10.1016/j.polymdegradstab.2015.07.024